Geomechanics and Engineering, *Vol. 34, No. 2 (2023) 115-124*
https://doi.org/10.12989/gae.2023.34.2.115

Investigation of three-dimensional deformation mechanisms of existing tunnels due to nearby basement excavation in soft clay

Wanchun Chen[1a], Lixian Tang[1b], Haijun Zhao[1c], Qian Yin[2d], Shuang Dong[1e], Jie Liu[1f], Zhaohan Zhu[3g] and Xiaodong Ni*[4]

[1]*China Construction Eight Engineering Division Rail Transit Construction Co., L.T.D., Nanjing, 210046 China*
[2]*Nanjing Metro, Nanjing, 210018, China*
[3]*School of Electrical Engineering, Southwest Jiaotong University, Chengdu, 611756, China*
[4]*Key Laboratory of Ministry of Education for Geomechanics and Embankment Engineering, Hohai University, Nanjing, 210024, China*

(*Received December 30, 2022, Revised March 5, 2023, Accepted March 14, 2023*)

Abstract. By conducting three-dimensional simulation with consideration of small-strain characteristics of soil stiffness, the effects of excavation geometry and tunnel cover to diameter ratio on deformation mechanisms of an existing tunnel located either at a side of basement or directly underneath the basement were systematically studied. Field measurements were used to verify the numerical model and model parameters. For basement excavated at a side of an existing tunnel, the maximum settlement and horizontal displacement of the tunnel are always observed at the tunnel springline closer to basement and tunnel crown, respectively, regardless of basement geometry. By increasing basement length and width by five times, the maximum movements of tunnel located at the side of basement and directly underneath the basement increase by 450% and 186%, respectively. Obviously, tunnel movements are more sensitive to basement length rather than basement width. For basement excavated at a side of an existing tunnel, tunnel movements at basement centerline become stable when basement length reaches 10 H_e (i.e., final excavation depth). Moreover, tunnel heaves due to overlying basement excavation become stable when the normalized basement length (L/H_e) is larger than 8.0. As tunnel cover to diameter ratio varies from 2.5 to 3.0, the maximum heave and tensile strain of tunnel due to overlying basement excavation decrease by up to 41.0% and 44.5%, respectively. If basement length is less than 8 H_e, the assumption of plane strain condition of basement-tunnel interaction grossly overestimates tunnel movements, and ignores tensile strain of tunnel along its longitudinal direction. Thus, three-dimensional numerical analyses are required to obtain a reasonable estimation of tunnel responses due to adjacent and overlying basement excavations in clay.

Keywords: basement excavation; basement length; basement width; three-dimensional deformation; tunnel

1. Introduction

Because of rapid growth in population, the subway becomes the main transportation in mega cities, such as Shanghai, London and Hong Kong. Currently, many subways have been constructed in those mega cities (e.g., Forth 2004, Marshall and Mair 2011, Klar *et al.* 2016, Cui *et al.* 2018, Sadique *et al.* 2022, Zaid 2021a, Zaid 2021b, Zaid 2021c). For convivences, it is not uncommon to construct basements for shopping malls or carparks at a side of or directly above an existing tunnel (e.g., Leung *et al.* 2000, Zheng *et al.* 2008, Devriendt *et al.* 2010, Khabbaz *et al.* 2019, Liang *et al.* 2021, Vinoth and Aswathy 2021, Ye *et al.* 2021, Zaid and Mishar 2021, Zaid and Shah, 2021, Zaid *et al.* 2022) or an existing pile (Meng *et al.* 2020, Cui *et al.* 2022, Cui *et al.* 2023, Kong *et al.* 2023a, Kong *et al.* 2023b, Zhou *et al.* 2023). As a result of basement excavation-induced stress changes in the ground, the existing tunnels undergo additional deformations and tensile strains. If basement excavation-induced additional deformation exceeds the allowable values, the serviceability and safety of existing tunnels may be affected.

By conducting field studies (e.g., Wen *et al.* 2010, Zhang *et al.* 2012, Li *et al.* 2018, Mahajan *et al.* 2019, Soomro *et al.* 2019), tunnel responses due to above and adjacent basement excavations were monitored. Because of basement excavation, the maximum settlement and heave of existing tunnels located at a side of and underneath basements were 11.0 mm and 14.2 mm, respectively. All those measured tunnel movements exceeded the allowable criterion of an existing tunnel given by Liu *et al.* (2011).

By conducting extensive centrifuge tests in dry sand, effects of relative basement-tunnel location, soil density and wall stiffness on tunnel responses were explored (e.g., Ng *et al.* 2013, Ng *et al.* 2015, Meng *et al.* 2023). It was found that much larger deformations were induced in an existing tunnel located underneath a basement rather than at side of

*Corresponding author, Professor
E-mail: cegeo2023@163.com
[a]MPhil
[b]MPhil
[c]MPhil
[d]Bachelor
[e]MPhil
[f]MPhil
[g]MPhil

ISSN: 2005-307X (Print), 2092-6219 (Online)

a basement. But this conclusion may be applicable for a tunnel located below the formation level of basement in sand. For an existing tunnel located at the side but above the formation level of basement in clays, basement excavation-induced maximum tunnel settlement was as high as 19.0 mm (Ge 2002). By conducting three-dimensional numerical parametric study in dry sand, Shi *et al.* (2015, 2019) found that basement-tunnel interaction along basement centerline could be simplified as plane strain condition as long as the basement length reached 10 times of the final excavation depth. In those studies, basements were mainly excavated in dry sand, which was different from ground stratum in Shanghai, London and Singapore. Thus, conclusions drawn from basement-tunnel interaction in dry sand may not be applicable for tunnel responses due to basement excavation in clays.

By conducting three-dimensional numerical analyses and centrifuge tests in soft clay, Huang *et al.* (2014) explored responses of an existing tunnel due to overlying basement excavation. As an increase in tunnel cover to diameter (*C/D*) ratio, basement excavation induced heave in the underlying tunnel decreased rapidly. By using Mindlin's solutions, Sun *et al.* (2019) proposed an analytical solution for estimating tunnel responses due to overlying basement excavation in dry sand. Using Pasternak foundation model, Huang *et al.* (2022) developed an analytical solution for estimating deformation of a segmental tunnel due to overlying basement excavation. Although basement excavation at a side of basement causing excessive tunnel movements (e.g., Ge 2002, Li *et al.* 2018, Liu *et al.* 2020, Bu *et al*. 2022), previous studies mainly focused on tunnel responses due to overlying basement excavation.

Current studies mainly focused on tunnel responses due to overlying basement excavation in dry sand. For basement excavated at a side of an existing tunnel, three-dimensional tunnel deformation mechanisms in soft clays were not fully understood. By conducting three-dimensional simulation with consideration of small strain soil stiffness, the effects of excavation geometry and tunnel cover to diameter ratio on deformation mechanisms of an existing tunnel located either at a side of basement or directly underneath basement were systematically studied.

2. Three-dimensional numerical modelling of basement-tunnel interaction in clay

2.1 Numerical analysis program

Fig. 1 shows a schematic view of basement-tunnel interaction considered in this study. A new basement was constructed at a side of or directly above an existing tunnel. The designed final excavation depth of the basement was 12 m, which was a typical value in practice. In order to ensure the serviceability and safety of the existing tunnel, diaphragm wall with a thickness of 0.8 m and three horizontal concrete props were designed to reduce basement excavation-induced lateral wall movements. To alleviate basement excavation-induced adverse effects on existing tunnels, soil within basement was reinforced to reduce

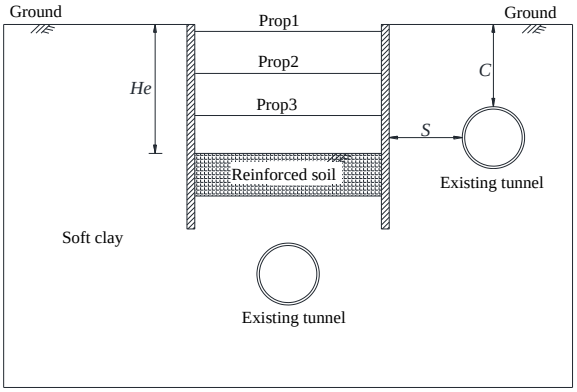

Fig. 1 The relative position between basement and existing tunnels

Table 1 Numerical analysis scheme of basement excavated at side of an existing tunnel

Normalized excavation length, L/H_e	Normalized excavation width, B/H_e	Clear distance between tunnel and basement, *S/D*	Tunnel cover to diameter ratio, *C/D*
2, 4, 6, 8, 10	2	0.5, 1.0	1.0
2	2, 4, 6, 8, 10	0.5, 1.0	1.0

Table 2 Numerical analysis scheme of basement excavated above an existing tunnel

Normalized excavation length, L/H_e	Normalized excavation width, B/H_e	Tunnel cover to diameter ratio, *C/D*
2, 3, 4, 5, 6, 7, 8, 9, 10	2, 3, 5	2.5, 3.0

basement excavation induced tunnel movements.

In the numerical parametric study, effects of basement geometry and relative position between basement and tunnel were explored. In practice, basements were normally constructed at least 3 m away from an existing tunnel. Moreover, the cover depth of an exiting tunnel was normally larger than 3.0 m. Previous studies have reported that excavation length or excavation width can be as high as 10 to 20 times of the final excavation depth. For basement constructed at a side of an existing tunnel, the normalized clear distances between basement and existing tunnel (*S/D*) were 0.5 and 1.0. Both the normalized excavation length (L/H_e) and excavation width (B/H_e) were varied from 2 to 10. In all these cases, the cover to tunnel diameter ratio (*C/D*) was controlled as 1.0.

For basement constructed directly above an existing tunnel, the normalized excavation length (L/H_e) and excavation width (B/H_e) were varied from 2 to 10 and 2 to 5, respectively. In reality, the outer diameter of shield tunnel was approximate 6 m, and tunnel cover to diameter ratio was in a range of 2.0 to 5.0 (e.g., Shi *et al.* 2022). To explore the effects of tunnel cover to diameter ratio (C/D) on tunnel responses, C/D ratios were varied from 2.5 to 3.0. In total, 72 numerical runs were conducted to investigate three-dimensional deformation mechanisms of an existing tunnel located either at a side of basement or directly underneath a basement in clays.

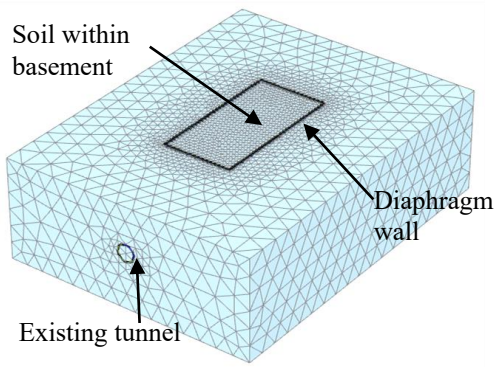

(a) All the finite element mesh

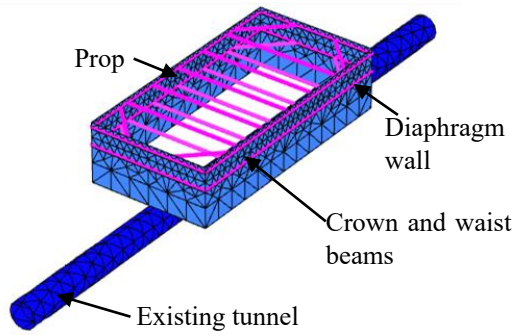

(b) Retaining wall and existing tunnel

Fig. 2 Three-dimensional numerical mesh of basement excavation above an existing tunnel

2.2 Finite element mesh and boundary conditions

Fig. 2 shows the three-dimensional finite element mesh of basement excavation above an existing tunnel. For this typical finite element mesh, the basement length (L), basement width (B) and final excavation depth (H_e) were 72, 24 and 12 m, respectively. As reported by previous studies, the influence zone of soil behind the retaining wall due to basement excavation was 4 times of the final excavation depth (Hsieh and Ou 1998). In this study, the clear distance between the retaining wall and mesh boundary was kept as 50 m, which was 4.2 times of the final excavation depth. Moreover, the distance between the tunnel invert and the bottom of mesh was 3 times of the final excavation depth, which was wider than the primary zone of ground deformation due to basement excavation in soft clays (Hsieh and Ou 1998). Thus, the model dimension was large enough to eliminate boundary effects on tunnel responses. A typical shield tunnel with an outer diameter of 6.2 m and a wall thickness of 0.35 m was simulated in this study. The total length of the retaining wall was 21 m, implying that the penetration ratio of the retaining wall was 0.75 m. To reduce basement excavation-induced soil and structure deformations, soil within basement was reinforced by jet grouting.

To considering the effects of joints on tunnel flexural stiffness, the shield tunnel was simulated by a continuous structure with a reduced stiffness. The tunnel joints were not directly simulated in the numerical analysis. This study aims to investigate three-dimensional deformation mechanisms due to nearby basement excavation. Thus, the conclusions drawn from this study was not affected by this simplification, and the comparative purpose of tunnel responses at different conditions were achieved.

Table 3 HSS model parameters of soft clay and cemented

Model Parameter	Soft clay	Cemented soil
Secant modulus, E_{50}^{ref} (MPa)	3.6	15
Tangent oedometric modulus, E_{oed}^{ref} (MPa)	4.3	15
Unloading–reloading modulus, E_{ur}^{ref} (MPa)	25.2	85
Modulus stress related power exponent, m	0.8	0.5
Effective cohesion, c' (kPa)	10	60
Effective friction angle, φ' (°)	25	25
Shear strain corresponding to initial shear modulus, $\gamma_{0.7}$ (10^{-4})	2.0	20.0
Initial shear modulus, G_0^{ref} (MPa)	100.8	170

Soil stratum was simulated by 10 nodded tetrahedron elements, retaining wall and existing tunnel were modeled by plate elements. Moreover, horizontal props, crown and waist beams were simulated by beam elements. The mesh size was halved until the computed tunnel responses was not affected by the mesh density. This three-dimensional mesh consisted of 102099 elements and elements and 150641 nodes. By using a computer with a ram memory of 32 GB, a numerical run took about two hours.

Impermeable interfaces were applied to the retaining wall and existing tunnel to ensure no leakage during basement excavation. In order to simulate the behaviors of the soil-structure interaction, positive and negative interfaces were applied to the tunnel and retaining wall. To obtain a reasonable estimation of tunnel responses due to adjacent or above basement excavations, the mesh density was refined at the location of the retaining wall and tunnel. Pin supports were applied to the four vertical sides of the finite element mesh, while pin supports were applied to the bottom of the mesh.

2.3 Constitutive model and model parameters

It is well-known that soil stiffness depends on stress and strain levels. In literature, basement excavation-induced shear strain in the soil commonly varied from 0.01% to 0.1% (e.g., Atkinson *et al.* 1990, Powrie *et al.* 1998, Chen *et al.* 2022). For soil strain within small strain level, soil stiffness decreased rapidly as an increase in the shear strain. Simple constitutive models (Mohr-Column and Cam-clay models) could not effectively capture the small strain soil stiffness, causing inaccurate prediction of ground and tunnel responses due to basement excavation. Thus, it is crucial to consider small strain soil stiffness in the analysis of basement-tunnel interaction. Since hardening soil model with small-strain stiffness (HSS) had the ability to model

small strain soil stiffness, this model was widely used to predict ground and structure responses due to basement and tunnel excavations.

In this study, an advanced constitutive soil model, namely hardening soil model with small strain stiffness (HSS), was used to simulate nonlinear soil behaviors. The governing soil parameters of the HSS model included soil secant modulus (E_{50}^{ref}), tangent oedometric modulus (E_{oed}^{ref}), unloading–reloading modulus (E_{ur}^{ref}), modulus stress related power exponent (m), initial shear modulus (G_0^{ref}), shear strain corresponding to initial shear modulus ($\gamma_{0.7}$), and strength parameters (c' and φ'). Based on the Plaxis user manual (Brinkgreve and Broere 2004), the secant modulus was equal to one-dimensional compression modulus (E_s), Tangent oedometric modulus was about 1.0~1.2 times of secant modulus, and unloading-reloading modulus was about 6-8 times of secant modulus. With known the one-dimensional compression modulus, other stiffness parameters could be determined.

By conducting one-dimensional compression test, the compression modulus of soil was obtained. Moreover, triaxial consolidated undrained tests were conducted to obtained strength parameters of soft clay and cemented clay. By using the relationships between compression modulus and other stiffness parameters suggested by Plaxis user manual, all the stiffness parameters of soft and cemented clays were obtained. Then, triaxial test results were used to verify all the stiffness parameters again. All the soil parameters of HSS model were summarized in Table 3.

Elastic model was used to simulate the behaviors of tunnel lining, retaining wall, internal props. The concrete grades of tunnel lining, retaining wall and internal props were C50, C35 and C30, corresponding to Young's moduli of 34.5, 31.5 and 30 GPa, respectively. The unit weight and Poisson's ratio of concrete were 25 kN/m^3 and 0.2, respectively. For the basement with a final excavation depth of 12 m, three levels of horizontal props made of concrete were designed with vertical and horizontal spacings of 3.5 and 8.0 m, respectively. The cross section of the first level of horizontal prop was 700 × 700 mm, while it was 800×1200 mm for both second and third levels of horizontal props.

2.4 Numerical modelling procedures

The numerical modelling procedures adopted in this study were the same as that in field. The key modelling procedures were listed as follows:

(1) The initial soil stress state was established by assuming K_0 condition, where K_0 was calculated by 1-sinφ', where φ' was internal frictional angle of soil at the critical state.

(2) Constructions of shield tunnel and retaining wall were modelled by activating the corresponding plate elements, respectively.

(3) Basement excavation was simulated in four consecutive steps. The ground water level was dewatered to 1.5 m, 5.0 m, 8.5 m and 12.0 m below ground surface, respectively.

(4) As long as the ground water level was dewatered to the target level, the above soil was removed to simulated basement excavation.

(5) After each soil layer was removed, the horizontal props were installed at 1.0 m above the excavation level.

(6) Upon completion of basement excavation, concrete base slab was simulated by activating the corresponding plate elements.

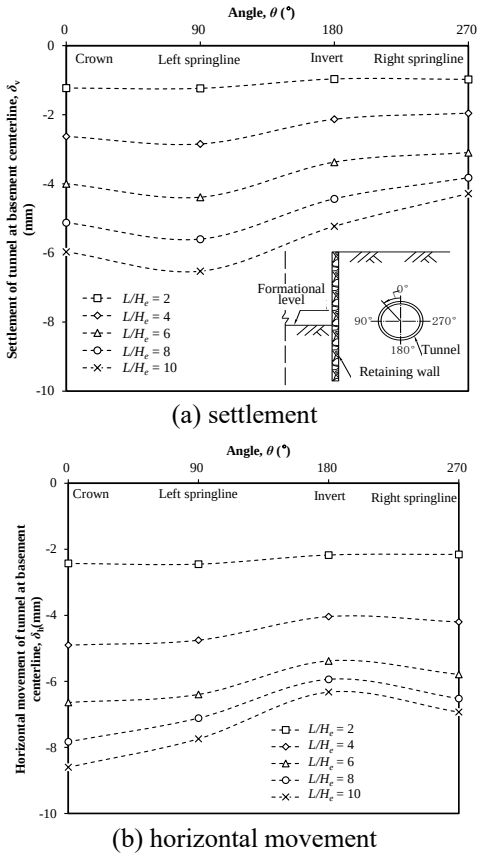

(a) settlement

(b) horizontal movement

Fig. 3 Effects of basement length on tunnel responses along the transverse direction

3. Effect of basement geometry on deformation mechanisms of an existing tunnel located at a side of basement

3.1 Effects of basement length on tunnel responses

3.1.1 Movements of tunnel along its transverse direction

Fig. 3(a) shows the effects of basement length on tunnel settlement at basement centerline. Positive and negative values denote heave and settlements, respectively. Because of stress relief caused by basement excavation, settlements are observed in the existing tunnel located at the side of the basement. θ is the central angle started from tunnel crown at an anticlockwise direction (i.e., details refer to the schematic diagram shown in Fig. 3). For a given normalized

basement length (L/H_e), tunnel settlement increases firstly followed by a slight decrease as an increase in the angle θ (i.e., from tunnel crown to spingling and invert). Since the left springling of existing tunnel is located closest to basement, tunnel settlement at this location is greatest. In contrary, tunnel settlement at the right springline is smallest since this location is the most far away from the basement.

Fig. 3(b) shows the effects of basement length on horizontal movement of existing tunnel along the basement centerline. Negative value denote tunnel moves toward basement, while positive value denote tunnel moves far away from basement. As a result of basement excavation, the existing tunnel moves toward basement. By increasing the angle θ, horizontal movements of existing tunnel also increase first followed by a slight decrease. But the greatest and smaller horizontal movements of tunnel lining are located at the tunnel crown and invert, respectively.

By increasing the normalized basement length (L/H_e) from 2.0 to 10.0, the maximum settlement and horizontal movement of existing tunnel due to adjacent basement excavation are always located at the left springline and crown, respectively. Thus, much more attention should be paid to left springline and crown for basement constructed at a side of an existing tunnel.

3.1.2 Movements of tunnel along its longitudinal direction

Fig. 4 shows the effects of basement length on settlement and horizontal movements of tunnel along its longitudinal direction. All the tunnel settlement (δ_v), horizontal movement (δ_h) and distance from tunnel centerline (X) are normalized by the final excavation depth (H_e). As expected, settlement and horizontal movement of tunnel due to adjacent basement excavation are symmetrical with respect to basement centerline. As an increase in the normalized distance from basement centerline, a rapid decrease in the settlement and horizontal movements of tunnel is observed. For basement excavated at 1.0 D away from the existing tunnel, basement excavation induced maximum tunnel settlements are 0.010% H_e, 0.024% H_e, 0.037% H_e, 0.048% H_e and 0.055% H_e, respectively, when the normalized basement lengths are 2.0, 4.0, 6.0, 8.0 and 10.0. Moreover, basement excavation-induced maximum horizontal movements in the existing tunnel are 0.020% H_e, 0.041% H_e, 0.055% H_e, 0.065% H_e and 0.072% H_e, respectively.

In following section, only the maximum tunnel responses at basement centerline are presented. Fig. 5 shows the maximum settlement and horizontal movement of existing tunnel due to adjacent basement excavation. Obviously, more stress relief within basement is occurred as an increase in basement length. Accordingly, maximum tunnel responses increase with the excavation length. The maximum settlement and horizontal movement increase as the normalized basement varies from 2 to 10, but at a reduced rate. If basement length is long enough, the basement-tunnel interaction at the basement centerline is close to plane strain condition.

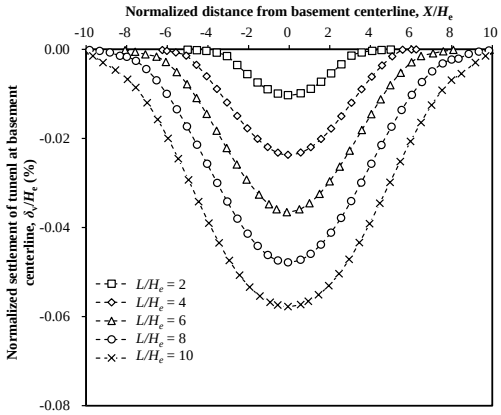

(a) settlement

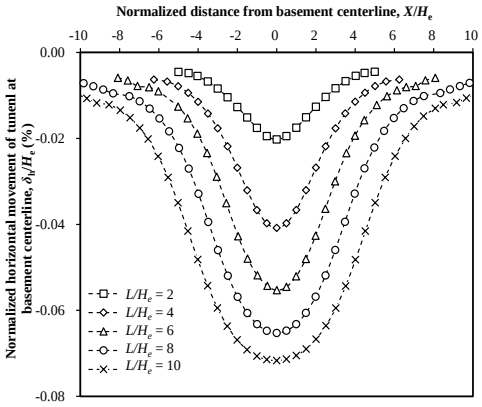

(b) horizontal movement

Fig. 4 Effects of basement length on tunnel responses along the longitudinal direction

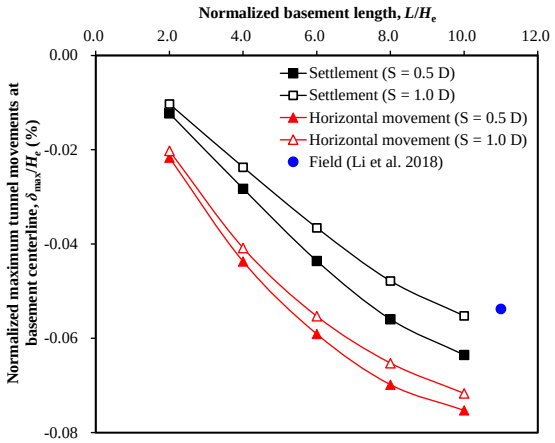

Fig. 5 Maximum settlement and horizontal movement of existing tunnel due to adjacent basement excavation with different excavation lengths

By increasing the normalized excavation length from 2.0 to 10.0, basement excavation-induced maximum settlement and horizontal movement in the existing tunnel increase by 4.3-4.5 and 2.4-2.6 times, respectively. For the model geometry considered in this study, excavation-induced maximum settlement and horizontal movement in the existing tunnel do not reach stable values even the normalized excavation length is larger than 10. By keeping

increasing the basement length, the basement-tunnel interaction at the basement centerline can reach the plane strain condition. Thus, settlement and horizontal movements of tunnel due to adjacent basement excavation with a short length ($L/H_e = 2$) are overestimated by up to 4.3 and 2.4 times if the basement-tunnel interaction is assumed as a plane strain condition. In other words, assumption of plane strain condition of basement-tunnel interaction grossly overestimates tunnel response, especially for basement with a relatively short length.

For tunnel located closer to basement, it suffers much larger stress relief, causing much larger tunnel movements. As the clear distance between the existing tunnel and retaining wall increases from 0.5 to 1.0, the maximum tunnel settlement and horizontal movement decrease by 4.8-6.5% and 13.0-16.1%, respectively. To ensure the serviceability and safety of the existing tunnel, the clear distance between the tunnel and basement should be strictly controlled in practice.

Field measurement is used to verify the computed results. Li *et al.* (2018) monitored settlement of an existing tunnel due to adjacent basement excavation. In this site, a basement with a final excavation depth of 18.6 m and a normalized excavation length of 11 was constructed at a clear distance of 1.3 D away from an existing tunnel. Because of basement excavation, a maximum settlement of 0.054% H_e is observed at the adjacent tunnel. Note that the measured maximum tunnel settlement is slightly smaller than the computed value of tunnel located at 1 D away from the basement. The discrepancies between the measured and computed results are probably due to different soil stratum and retaining structure. In general, the computed tunnel movements are comparable to the measured results. It implies that the soil model and model parameters used in this study are reasonable.

3.2 Effects of excavation width on tunnel responses

Fig. 6 shows the effects of basement width on tunnel responses at the basement centerline. For the basement widths considered in this study, locations of the maximum tunnel responses are the same as that shown in Fig. 3. The maximum and minimum tunnel settlements are located at the left and right springlines, respectively. Moreover, the greatest and smallest horizontal movements are induced at the tunnel crown and invert, respectively. It is indicated that the maximum elongation and compression of the tunnel lining is independent of basement geometry. For basement excavated at a side of an existing tunnel, much more attention should be paid to settlement at the tunnel crown and horizontal movement at the springline located closer to the basement.

As shown in Fig. 4, the maximum tunnel responses are observed along the basement centerline. Thus, only the maximum tunnel responses along the basement centerline are presented in following section. Fig. 7 shows variations of the maximum settlement and horizontal movements of existing tunnel due to adjacent basement excavation. At a given excavation length and a clear distance between the

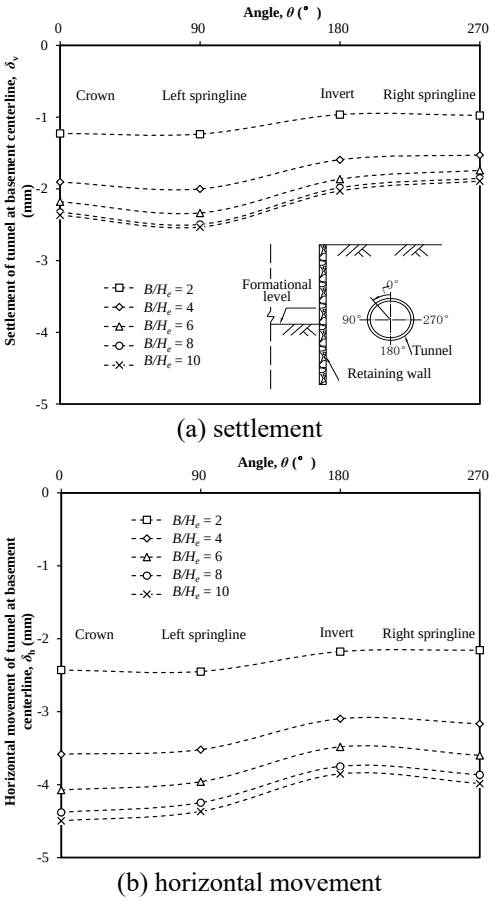

(a) settlement

(b) horizontal movement

Fig. 6 Effects of basement width on tunnel responses along the transverse direction

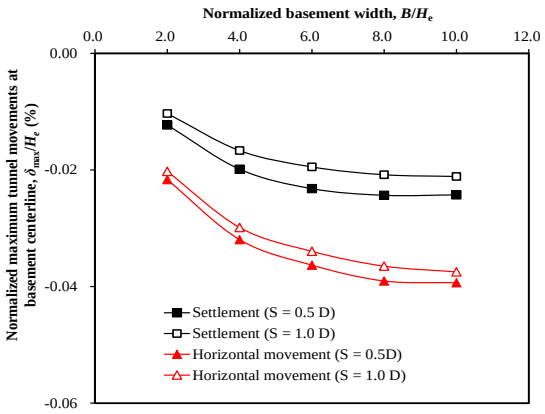

Fig. 7 Maximum settlement and horizontal movement of existing tunnel due to adjacent basement excavation with different excavation widths

tunnel and basement, the maximum tunnel responses due to basement excavation increase with excavation width, but at a reduced rate. For the existing tunnel located 1.0 D away from the basement, basement excavation-induced maximum tunnel settlements are 0.010% H_e, 0.017% H_e, 0.019% H_e, 0.020% H_e and 0.021% H_e, respectively, when the normalized basement lengths are 2.0, 4.0, 6.0, 8.0 and 10.0. Moreover, basement excavation-induced maximum horizontal movements in the existing tunnel are 0.020% H_e,

0.030% H_e, 0.034% H_e, 0.036% H_e and 0.037% H_e respectively. When the normalized basement width is larger than 8, basement excavation-induced tunnel responses reach stable values. As an increase in the basement width, three-dimensional effects on constraining soil and retaining wall deformations are gradually reduced. Consequently, soil behind the retaining wall has less resistances to slide into basement, causing much larger tunnel movements.

As the normalized basement width (B/H_e) increases from 2.0 to 1.0, basement excavation-induced maximum settlement and horizontal movement of existing tunnel increase by 100-110% and 77-85%, respectively. However, the increases in tunnel settlement and horizontal movement are up to 450% and 260%, respectively, when the normalized basement length (L/H_e) increases from 2.0 to 1.0. Obviously, the effects of basement length on tunnel responses are much more prominent than basement width. If possible, designers should reduce basement length along the longitudinal direction to ensure the serviceability of existing tunnels. During the construction of basement excavation, installation of partition walls can divide a long basement into several short basements with small basement length. Moreover, stagged excavation technique is suggested to reduce basement excavation-induced adverse effects on adjacent tunnels.

4. Effect of excavation geometry on deformation mechanisms of an existing tunnel located underneath basement centerline

4.1 Maximum tunnel heave

Fig. 8 shows the maximum heave induced in the existing tunnel due to basement excavation with different geometries. The maximum tunnel settlement, basement length and basement width are normalized by the final excavation depth. As expected, the maximum heave induced in the tunnel increases with the basement length. For tunnel cover to diameter ratio (C/D) of 2.5 and normalized excavation length (L/H_e) of 10, the maximum tunnel heave increases by 39% as the normalized basement width (B/H_e) varies from 2.0 to 3.0. By further increasing the basement width (B) to 5.0 H_e, the maximum tunnel heave only increases by 4.2%. For the normalized basement widths of 2.0, 3.0 and 5.0, the maximum tunnel heaves due to basement excavation increases by 110%, 160% and 186%, respectively, when the normalized basement length varies from 1.0 to 10.0. Obviously, the tunnel heave due to overlying basement excavation is more sensitive to basement length rather than basement width. Note that the tunnel heave exceeds allowable movement limit (i.e., 10 mm given by Liu *et al*. (2011)), countermeasures such as jet grouting and anti-uplift piles are suggested to alleviate basement excavation-induced adverse effects.

When the normalized excavation length (L/H_e) reaches 8.0, the tunnel heave reaches stable values. It implies that the basement-tunnel interaction along the basement centerline reaches plane strain condition when the normalized basement length is larger than 8.0. Thus, tunnel

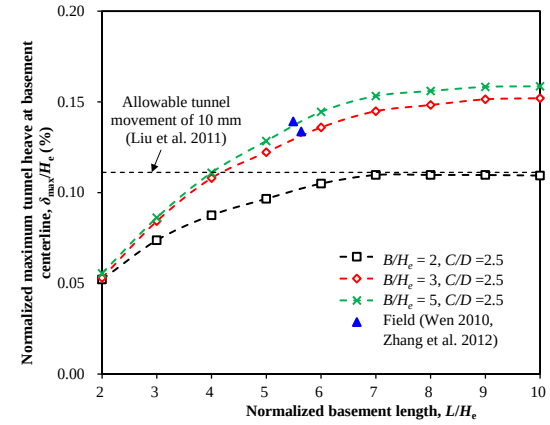

(a) C/D = 2.5

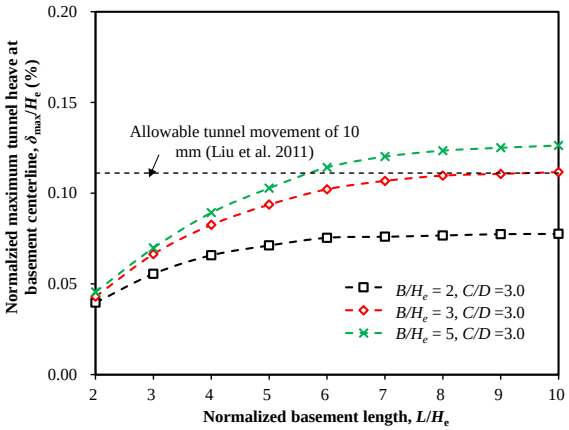

(b) C/D = 3.0

Fig. 8 Effects of basement geometry on maximum tunnel heave

heave is expected to be overestimated by 1.1-1.9 times if a short basement (L/H_e=2) is assumed as plane strain condition. It is indicated that again plane strain assumption of basement-tunnel interaction can grossly overestimated tunnel heave due to basement excavation. A real three-dimensional numerical analysis is required to obtain a reasonable estimation of the maximum tunnel heave due to basement excavation in clay.

By conducting field study, Zhang *et al.* (2012) and Wen (2010) monitored the tunnel heave due to overlying basement excavation in soft clay. In those two studies, basements are constructed directly above existing tunnels with cover depth to diameter ratios (C/D) of 2.30 and 2.42.

The normalized width of these two basements is larger than 5, and the normalized basement lengths are 5.5 and 5.6, respectively. Upon completion of the basement excavation, the measured maximum tunnel heaves are 0.139% H_e ad 0.134% H_e, respectively. As shown in Figure 8(a), the field measurements are in a good agreement with the computed results, indicating that the soil model and model parameters adopted in this study are reasonable.

When the normalized basement widths (B/H_e) are 2.0, 3.0 and 5.0, basement excavation-induced maximum heaves in shallowly buried tunnel (C/D = 2.5) are 41.0%, 36.0% and 26.0% larger than that of deeply buried tunnel (C/D =

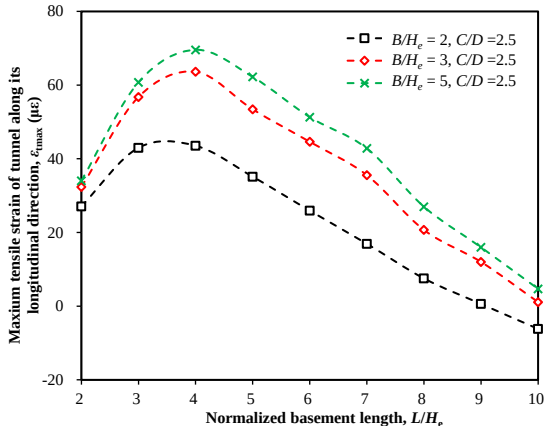

(a) C/D = 2.5

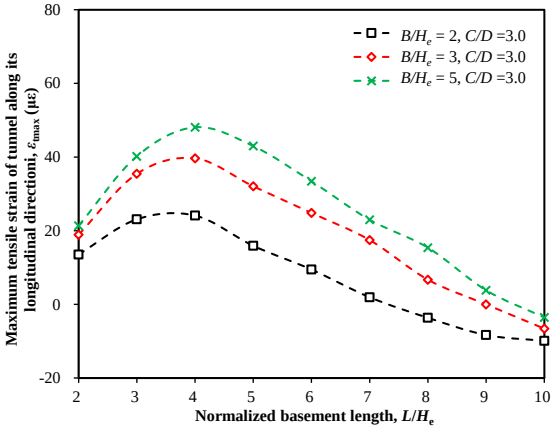

(b) C/D = 3.0

Fig. 9 Effects of basement geometry on maximum tensile strain of tunnel along its longitudinal direction

3.0). This is because shear stiffness of soil surrounding a deep tunnel is much larger than that surrounding a shallow tunnel. At a given vertical stress relief, large soil stiffness causes small soil and tunnel movements.

4.2 Maximum tensile strain of tunnel along its longitudinal direction

Fig. 9 shows the effects of basement geometry on maximum tensile strain of tunnel along its longitudinal direction. As the normalized basement length (L/H_e) increases from 2 to 4, a clear increase in the maximum tensile strain of tunnel along its longitudinal direction is observed. By further increasing the normalized basement length (L/H_e), the maximum tensile strain induced in the existing tunnel decreases dramatically. When the basement length reaches 10 times of the final excavation depth, tensile strain induced in the tunnel along the basement centerline is close to zero. For plane strain assumption of basement-tunnel interaction, there is no any tensile strain of tunnel along its longitudinal direction. Thus, the basement-tunnel interaction at the basement centerline cannot simplified as a plane strain condition unless the normalized basement length is larger than 10.

As an increase in the basement width, basement excavation-induced tensile strain in the tunnel is also increased, but at a reduced rate. For tunnel with cover depth to diameter ratios (C/D) of 2.5 and 3.0, the maximum tensile strains of tunnel along its longitudinal direction increase by 59.8% and 99.5%, respectively, when the normalized basement width increases from 2.0 to 5.0.

When tunnel cover to diameter ratio is 2.5, basement excavation-induced maximum tensile strains in the tunnel are 43.5, 63.6 and 69.6 με, respectively, for normalized basement widths (B/H_e) of 2.0, 3.0 and 5.0. For basement with a relatively short length, excavation-induced tensile strain in the existing tunnel cannot be ignored. By increasing tunnel cover to diameter ratio from 2.5 to 3.0, basement excavation-induced maximum tensile strain in the tunnel decreases by 30.9%-44.5%. This is because soil surrounding a deeper tunnel has larger stress and stiffness. At a given vertical stress relief, soil heave surrounding a deeper tunnel is expected to be smaller, resulting in smaller tunnel heave.

7. Conclusions

In this study, deformation mechanisms of an existing tunnel due to adjacent and overlying basement excavations in soft clay are explored by three-dimensional numerical analyses. Based on the computed results, the major conclusions are drawn as follows:

(1) For basement excavated at a side of an existing tunnel, the tunnel moves downward and toward to basement. The maximum elongation and compression of tunnel lining are always located at the springline closer to basement and crown, regardless of basement geometry.

(2) As basement width increases by 5 times, excavation-induced maximum settlement, horizontal movement in adjacent tunnel and heave of underlying tunnel increases by 110%, 85% and 41%, respectively. Moreover, the maximum settlement, horizontal movement of adjacent tunnel and heave of underlying tunnel increases by 450%, 260% and 186%, respectively, as the basement length increases by 5 times. It is indicated that tunnel responses due to adjacent and overlying basement excavations are more sensitive to basement length.

(3) For basement excavated at a side of an existing tunnel, excavation-induced maximum tunnel settlement and horizontal movement decrease by 4.8-6.5% and 13.0-16.1%, respectively, as the clear distance between the tunnel and retaining wall increase from 0.5 to 1.0. For basement excavated above an existing tunnel, the maximum heave and tensile strain of tunnel are reduced by up to 41.0% and 44.5%, respectively, as tunnel cover to diameter ratio varies from 2.5 to 3.0.

(4) As an increase in basement length or width, tunnel deformations along basement centreline gradually reach stable values. When the normalized basement length is 10, excavation induced settlement and horizontal movement in adjacent tunnel become stable. Moreover, the tunnel heave due to overlying basement excavation become stable when the normalized basement length reaches 8.

(5) By simplifying a short basement as a plane strain problem, excavation-induced maximum settlement, horizontal movement of an adjacent tunnel and heave of underlying

tunnel are overestimated as high as 450%, 260% and 186%, respectively. If excavation length does not exceed 8 H_e (final excavation depth), the assumption of plane strain condition of basement-tunnel interaction grossly overestimates tunnel movements, and ignores tensile strain of tunnel along its longitudinal direction.

Acknowledgments

This work was supported by the National Natural Science Foundation of China (51779083) and the Zhejiang Engineering Research Center of Intelligent Urban Infrastructure (IUI2022-ZD-02).

References

Atkinson, J.H., Richardson, D. and Stallebrass, S.E. (1990), "Effect of recent stress history on the stiffness of overconsolidated soil", *Géotechnique*, **40**(4), 531-540. https://doi.org/ 10.1680/geot.1990.40.4.531.

Brinkgreve, R.B.J. and Broere, W. (2004), PLAXIS 3D Tunnel Version 2, PLAXIS by, Netherlands.

Bu, F.M., Yu, W.R., Chen, L. and Wu, E.R. (2022), "Investigation of three-dimensional deformation mechanisms of box culvert due to adjacent deep basement excavation in clays", *Geomech. Eng.*, **30**(6), 565-577. https://doi.org/10.12989/gae.2022.30.6.565.

Chen, L.A., Pei, W.W., Yang, Y.H. and Guo, W.L. (2022), "Three-dimensional numerical parametric study of shape effects on multiple tunnel interactions", *Geomech. Eng.*, **31**(3), 237-248. https://doi.org/ 10.12989/gae.2022.31.3.237.

Cui, C.Y., Meng, K., Wu, Y.J., Chapman, D. and Liang, Z.M. (2018), "Dynamic response of pipe pile embedded in layered visco-elastic media with radial inhomogeneity under vertical excitation", *Geomech. Eng.*, **16**(6), 609-618. https://doi.org/10.12989/gae.2018.16.6.609.

Cui, C.Y., Liang, Z.M., Xu, C.S., Xin, Y. and Wang, B.L (2023), "Analytical solution for horizontal vibration of end-bearing single pile in radially heterogeneous saturated soil", *Appl. Math. Model.*, **116**, 65-83. https://doi-org/10.1016/j.apm.2022.11.027.

Cui, C.Y., Meng, K., Xu, C.S., Wang, B.L. and Xin, Y. (2022), "Vertical vibration of a floating pile considering the incomplete bonding effect of the pile-soil interface", *Comput. Geotech.*, **150**, 104894. https://doi.org/10.1016/j.compgeo.2022.104894.

Devriendt, M., Doughty, L., Morrison, P. and Pillai, A. (2010), "Displacement of tunnels from a basement excavation in London", *Proceedings of the Institution of Civil Engineers-Geotechnical Engineering*, **163**(3), 131-145. https://doi.org/10.1680/geng.2010.163.3.131.

Forth, R.A. (2004), "Groundwater and geotechnical aspects of deep excavations in Hong Kong", *Eng. Geol*., **72**(3-4), 253-260. https://doi.org/10.1016/ j.enggeo.2003.09.003.

Ge, X.W. (2002), Response of a shield-driven tunnel to deep excavations in soft clay, Ph.D thesis, Department of Civil and Environmental Engineering, The University of Hong Kong Science and Technology, HKSAR.

Hsieh, P.G. and Ou, C.Y. (1998), "Shape of ground surface settlement profiles caused by excavation", *Can. Geotech. J.*, **35**(6), 1004-1017. https://doi.org/ 10.1139/cgj-35-6-1004.

Huang, X., Huang, H.W. and Zhang, D.M. (2014), "Centrifuge modelling of deep excavation over existing tunnels", *Proceedings of the ICE-Geotechnical Engineering*, **167**(2), 3-18. https://doi.org/ 10.1680/geng.11.00045.

Huang, S., Chen, Z., Xie, Y. and Lin, Z. (2022), "A variational approach to the analysis of excavation-induced vertical deformation in a segmental tunnel", *Tunn. Undergr. Sp. Tech.*, **122**, 104342. https://doi.org/10.1016/j.tust.2021.104342.

Khabbaz, H., Gibson, R. and Fatahi, B. (2019), "Effect of constructing twin tunnels under a building supported by pile foundations in the Sydney central business district", *Undergr. Space*, **4**(4), 261-276. https://doi.org/10.1016/j.undsp.2019.03.008.

Klar, A., Elkayam, I. and Marshall, A.M. (2016), "Design oriented linearequivalent approach for evaluating the effect of tunneling on pipelines", *J. Geotech. Geoenviron. Eng.*, **142**(1), 04015062. https://doi.org/10.1061/(ASCE)GT.1943-5606.0001376.

Kong, G.Q., Hu, S.J. and Yang Q. (2023a), "Uncertainty method and sensitivity analysis to assess building energy of underground metro station", *Sustain. Cities Soc.*, **92**, 104504. https://doi.org/10.1016/j.scs.2023. 104504.

Kong, G.Q., Fang, J.C., Lv, Z.X. and Yang, Q. (2023b), "Effects of pile and soil properties on thermally induced mechanical responses of energy piles", *Comput. Geotech.*, **154**, 105176. https://doi.org/10.1016/ j.compgeo. 2022.105176.

Li, C.W., Li, W. and Liang, Z.R. (2018), "Design and analysis on synchronous construction of deep foundation pit on both sides of tunnels in soft soils", *Chinese J. Undergr. Sp. Eng.*, **14**(S1), 197-203. https://doi.org/10.16285/j.upe.2018.S1.031.

Leung, C.F., Chow, Y.K. and Shen, R.F. (2000), "Behavior of pile subject to excavation-induced soil movement", *J. Geotech. Geoenviron. Eng.*, **126**(11), 947-954. https://doi.org/10.1061/(ASCE)1090-0241(2000)126:11(947).

Liu, B., Zhang, D.W., Yang, C. and Zhang, Q.B. (2020), "Long-term performance of metro tunnels induced by adjacent large deep excavation and protective measures in Nanjing silty clay", *Tunn. Undergr. Sp. Tech.*, **95**, 103147. https://doi.org/10.1016/j.tust.2019.103147.

Liu, H.L., Li, P. and Liu, J.Y. (2011), "Numerical investigation of underlying tunnel heave during a new tunnel construction", *Tunn. Undergr. Sp. Tech.*, **26**(2), 276-283. https://doi.org/10.1016/ j.tust.2010.10.002.

Liang, R.C., Wu, J., Sun, L.W., Shen, W. and Wu, W.B. (2021), "Performances of adjacent metro structures due to zoned excavation of a large-scale basement in soft ground", *Tunn. Undergr. Sp. Tech.*, **117**, 104123. https://doi.org/10.1016/j.tust.2021.104123.

Mahajan, S., Ayothiraman, R. and Sharma, K.G. (2019), "A parametric study on effects of basement excavation and foundation loading on underground metro tunnel in soil", *Indian Geotech. J.*, **49**, 667–686. https://doi.org/10.1007/s40098-019-00361-x.

Marshall, A.M. and Mair, R.J. (2011), "Tunneling beneath driven or jacked end-bearing piles in sand", *Can. Geotech. J.*, **48**(12), 1757-1771. https://doi.org/ 10.1139/t11-067.

Meng, F.Y., Chen, R.P., Liu, Y., Wu, H.N. and Cheng, H.Z. (2023), "Impacts of reinforced wall on nearby excavation-induced ground and tunnel responses: a centrifugal and numerical study", *Tunn. Undergr. Sp. Tech.*, **132**, 104903. https://doi.org/10.1016/j.tust.2022.104903.

Meng, K., Cui, C.Y., Liang, Z.M., Li, H.J. and Pei, H.F. (2020), "A new approach for longitudinal vibration of a large-diameter floating pipe pile in visco-elastic soil considering the three-dimensional wave effects", *Comput. Geotech.*, **128**, 103840. https://doi.org/10.1016/j.compgeo.2020.103840.

Ng, C.W.W., Shi, J.W. and Hong, Y. (2013), "Three-dimensional centrifuge modelling of basement excavation effects on an existing tunnel in dry sand", *Can. Geotech. J.*, **50**(8), 874-888. https://doi.org/10.1139/cgj-2012-0423.

Ng, C.W.W., Shi, J.W., Mašín, D., Sun, H.S. and Lei, G.H. (2015), "Influence of sand density and retaining wall stiffness on the

three-dimensional responses of a tunnel to basement excavation", *Can. Geotech. J.*, **52**(8), 1811-1829. https://doi.org/ 10.1139/ cgj-2014-0150.

Powrie, W., Pantelidou, H. and Stallebrass, S.E. (1998), "Soil stiffness in stress paths relevant to diaphragm walls in clay", *Géotechnique*, **48**(4), 483-494. https://doi.org/10.1680/geot.1998.48.4.483.

Sadique, M.R., Zaid, M. and Alam, M.M. (2022), "Rock tunnel performance under blast loading through finite element analysis", *Geotech. Geol. Eng*., **40**, 35-56. https://doi.org/10.1007/s10706-021-01879-9.

Shi, J.W., Ng, C.W.W. and Chen, Y.H. (2015), "Three-dimensional numerical parametric study of the influence of basement excavation on existing tunnel", *Comput. Geotech.*, **63**, 146-158. https://doi.org/10.1016/j.compgeo.2014.09.002.

Shi, J.W., Fu, Z.Z. and Guo, W.L. (2019), "Investigation of geometric effects on three-dimensional tunnel deformation mechanisms due to basement excavation", *Comput. Geotech.*, **106**, 108-116. https://doi.org/ 10.1016/j.compgeo.2018.10.019.

Shi, J.W., Chen Y.H., Lu, H., Ma, S.K. and Ng, C.W.W. (2022), "Centrifuge modeling of the influence of joint stiffness on pipeline response to underneath tunnel excavation", *Can. Geotech. J.*, **59**(9), 1568-1586. https://doi.org/10.1139/cgj-2020-0360.

Soomro, M. A., Saand, A., Mangi, N., Mangnejo, D.A., Karira, H. and Liu, K. (2019), "Numerical modelling of effects of different multipropped excavation depths on adjacent single piles: comparison between floating and end-bearing pile responses", *Eur. J. Environ. Civil Eng.*, **25**(14), 2592-2622. https://doi.org/10.1080/19648189.2019.1638312.

Sun, H., Chen, Y., Zhang, J. and Kuang, T. (2019), "Analytical investigation of tunnel deformation caused by circular foundation pit excavation", *Comput. Geotech.*, **106**, 193-198. https://doi.org/10.1016/ j.compgeo.2018.11.001.

Vinoth, M. and Aswathy, M.S. (2021), "Behaviour of existing tunnel due to adjacent excavation-a review", *Int. J. Geotech. Eng*., **16**(9), 1132-1151. https://doi.org/10.1080/19386362.2021. 1952800.

Ye, S.H., Zhao, Z.F. and Wang, D.Q. (2021), "Deformation analysis and safety assessment of existing metro tunnels affected by excavation of a foundation pit", *Undergr. Space*, **6**, 4211-431. https://doi.org/10.1016/j.undsp. 2020.06.002.

Wen, S.L. (2010), "Construction technology of deep open excavation above running metro tunnels", *Chinese J. Geotech. Eng.*, **32**(2), 451-454. https://doi.org/10.16285/j.rsm.2010.S2.031.

Zaid, M. (2021a), "Dynamic stability analysis of rock tunnels subjected to impact loading with varying UCS", *Geomech. Eng*., **24**(6), 505-518. https://doi.org/10.12989/gae.2021.24.6.505.

Zaid, M. (2021b), "Three-dimensional finite element analysis of urban rock tunnel under static loading condition: effect of the rock weathering", *Geomech. Eng*., **25**(2), 99-109. https://doi.org/10.12989/gae.2021.25.2.099.

Zaid, M. (2021c), "Preliminary study to understand the effect of impact loading and rock weathering in tunnel constructed in quartzite", *Geotech. Geol. Eng*., https://doi.org/10.1007/s10706-021-01948-z.

Zaid, M. and Mishra, S. (2021), "Numerical analysis of shallow tunnels under static loading: a finite element approach", *Geotech. Geol. Eng*., **39**(3), 2581-2607. https://doi.org/10.1007/s10706-020-01647-1.

Zaid, M., and Shah, I.A. (2021). "Numerical analysis of himalayan rock tunnels under static and blast loading". Geotechnical and Geological Engineering, 39, 5063–5083. https://doi.org/10.1007/s10706-021-01813-z

Zaid, M., Sadique, M.R. and Alam, M.M. (2022), "Blast resistant analysis of rock tunnel ssing Abaqus: effect of weathering", *Geotech. Geol. Eng*., **40**, 809-832. https://doi.org/10.1007/s10706-021-01927-4.

Zhang, J.F, Wang, J.H., Chen, J.J. and Hou, Y.M. (2012), "3-D FEM back-analysis of an oversize and deep excavation", *J. Shanghai Jiaotong Univ.*, **46**(1), 42-46. https://doi.org/10.16183/j.cnki.jsjtu.2012. 01.010.

Zheng, G. and Wei, S.W. (2008), "Numerical analysis of influence of overlying pit excavation on existing tunnels", *J. Central South Univ. Tech.*, **15**(2), 69-75. https://doi.org/10.1007/s11771-008-0438-4.

Zhou, Y., Kong, G.Q. and Li, J.J. (2023), "Performances of belled pile influenced by pile head freedom response to a cooling-heating cycle", *J. Geotech. Geoenviron. Eng.*, **149**(2), 04022133. https://doi.org/10.1061/JGGEFK.GTENG-10407.

GC